

## Regenerating LiFePO<sub>4</sub>/C using recycled LiH<sub>2</sub>PO<sub>4</sub> as raw material

Weihao Liu<sup>a</sup>, Xianbiao Chen<sup>b</sup>, Wenhua Zhang<sup>c\*</sup>, Fang Dai<sup>d</sup>, Shuai Wang<sup>e</sup>,  
Wang Peng<sup>f</sup>, Jie Zeng<sup>g</sup>, Zhe Chen<sup>h</sup>, Yinbao Miao<sup>i</sup> and Jia Liu<sup>j</sup>

School of Electrical Engineering, Nanchang Institute of Technology, Nanchang 330029, China.

<sup>a</sup>mookmoon914@yeah.net, <sup>b</sup>1965445606@qq.com, <sup>c\*</sup>2015994552@nit.edu.cn, <sup>d</sup>3952078@qq.com,  
<sup>e</sup>936074671@qq.com, <sup>f</sup>pengwang@163.com, <sup>g</sup>1052316946@qq.com, <sup>h</sup>350018127@qq.com,  
<sup>i</sup>3046523956@qq.com, <sup>j</sup>704604371@qq.com.

**Abstract.** In order to achieve low-cost regeneration of waste lithium iron phosphate electrode sheets, this paper uses LiH<sub>2</sub>PO<sub>4</sub> recovered by acid leaching method as raw material to regenerate LiFePO<sub>4</sub>/C, and further explores the effect of temperature on the electrochemical performance of regenerated LiFePO<sub>4</sub>/C. Through material structure characterization, it was found that the characteristic peaks of the recovered LiH<sub>2</sub>PO<sub>4</sub> corresponded one-to-one with the standard card, indicating a high degree of crystallinity, no obvious impurities, high purity, and complete crystal structure. When the temperature is 750°C, the lithium iron ratio is 1.03, and the conductive carbon black content is 5% of the mixture mass fraction, the regenerated LiFePO<sub>4</sub>/C exhibits the best electrochemical performance, with a first week discharge specific capacity of 125.7mAh/g at a rate of 0.1C; At 1C magnification, the first week discharge specific capacity is 106.2mAh/g, and after the 100th week, the discharge specific capacity is 93.1mAh/g, with a capacity retention rate of 87.7%. The cost of raw materials used is relatively low compared to other processes, and the regenerated LiFePO<sub>4</sub>/C produced by this process has the advantage of low price, making it more suitable for the mid to low-end energy storage market.

**Keywords:** LiH<sub>2</sub>PO<sub>4</sub>; LiFePO<sub>4</sub>/C; electrochemical.

### 1. Introduction

In recent years, lithium-ion batteries have been widely used as new energy storage devices in various fields such as portable electronic products, electric vehicles, and large-scale energy storage systems[1]. Among them, olivine type LiFePO<sub>4</sub> cathode material has attracted great attention since it was first discovered by Good Nough et al[2]. in 1997 due to its advantages of good cycling performance[3], high safety, and green environmental protection, and has successfully achieved large-scale commercial application. According to statistics, the domestic production of LiFePO<sub>4</sub> power batteries reached 27.7GW·h in 2019, accounting for 32.4% of the total production of power batteries[4]. Power batteries are generally retired due to capacity degradation after 8 to 10 years of use[5, 6]. It is expected that by 2030, approximately 6 million electric vehicle battery packs will be retired each year[7], with LiFePO<sub>4</sub> batteries accounting for a large proportion. If waste LiFePO<sub>4</sub> batteries are not properly recycled and treated, on the one hand, it will seriously pollute the atmosphere and water and soil resources[8], damage the ecosystem, and harm human health; On the other hand, it will cause waste of resources such as lithium, iron, and phosphorus. China's lithium resource reserves only account for 7% of the world's total[9-11], and its external dependence is high. If electrode materials are not recycled and reused, it will limit the sustainable development of the electric vehicle industry in the long run[12, 13]. In addition, recycling waste power batteries can also generate huge economic benefits. According to estimates, the market space for power battery recycling is expected to exceed 60 billion yuan from 2019 to 2025. Therefore, whether from an environmental or economic perspective, it is of great significance to carry out the recycling and reuse of waste LiFePO<sub>4</sub> batteries. In this context, this article reviews the research progress on the recycling and reuse of waste LiFePO<sub>4</sub> electrode materials in recent years, and focuses on the research work of our research group in the recycling and regeneration of waste LiFePO<sub>4</sub> cathode materials

## 2. Preparation and characterization of $\text{LiH}_2\text{PO}_4$ recovery

### 2.1 Preparation of $\text{LiH}_2\text{PO}_4$ from $\text{LiFePO}_4$ cathode material obtained from separation

In order to recover the raw material  $\text{LiH}_2\text{PO}_4$  for regeneration of  $\text{LiFePO}_4$ , the specific experimental operation process is shown in Figure 1. The specific operation is as follows: 5g of waste  $\text{LiFePO}_4$  cathode material is put into a 500mL beaker, 200mL of 0.5mol/L  $\text{H}_3\text{PO}_4$  solution and 6g of 30vol% hydrogen peroxide are added, and stirred at 300r/min for 4h at room temperature to separate undissolved impurities such as activated carbon and PVDF. The solution is heated and refluxed at  $85^\circ\text{C}$  for 12h, and a large amount of white flocculent precipitate is generated. After the reaction is completed, the precipitate is filtered to obtain an acid solution containing a large amount of  $\text{Li}^+$  and a small amount of  $\text{Fe}^{3+}$ . A quantitative amount of  $\text{LiOH}\cdot\text{H}_2\text{O}$  is added to the solution. White solid powder is continuously stirred to accelerate dissolution. When the pH value is adjusted to 7, stop adding and heat at  $90^\circ\text{C}$  for 1 hour. During this time, a large amount of white precipitate  $\text{Li}_3\text{PO}_4$  is generated. After the reaction is completed, wash and dry the white precipitate  $\text{Li}_3\text{PO}_4$ . The  $\text{Li}_3\text{PO}_4$  precipitation is shown in Figure 2(a). After drying, the  $\text{Li}_3\text{PO}_4$  was ground and weighed to a mass of 5.2g. Using the same experimental process as NaOH as the impurity removal agent, the  $\text{Li}_3\text{PO}_4$  obtained was only 2.4g in mass. The reason is that  $\text{LiOH}\cdot\text{H}_2\text{O}$  introduced  $\text{Li}^+$  into the solution during the dissolution of the acid solution, indirectly increasing the yield of the raw material.

Under normal temperature and pressure conditions, 1mol/L  $\text{H}_3\text{PO}_4$  solution was prepared and reacted with the  $\text{Li}_3\text{PO}_4$  obtained in the previous step, with a molar ratio of  $\text{Li}_3\text{PO}_4:\text{H}_3\text{PO}_4=1:2$ . The solution was heated to  $90^\circ\text{C}$  until the water was dried. Due to the low solubility of  $\text{LiH}_2\text{PO}_4$  in anhydrous ethanol<sup>[14]</sup>, an equal amount of anhydrous ethanol was added to the solution for solvent displacement, resulting in a large amount of white precipitate. After cooling to room temperature, a circulating vacuum pump was used for filtration. The solution was washed several times with anhydrous ethanol and dried at  $105^\circ\text{C}$  for 2 hours to obtain  $\text{LiH}_2\text{PO}_4$  white powder, as shown in Figure 2(b).

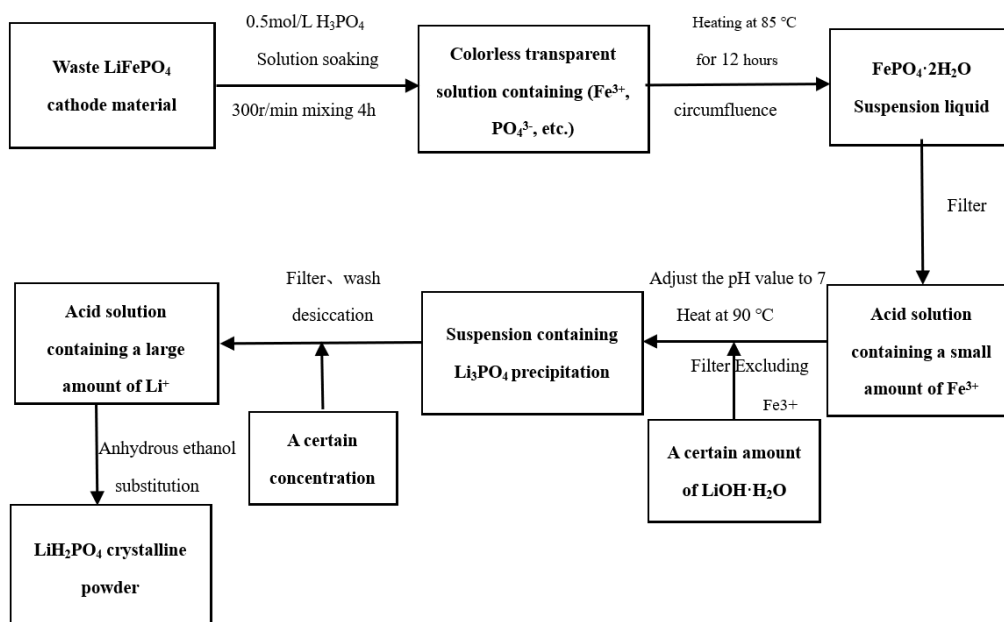


Figure 1. Process flow diagram for recycling  $\text{LiH}_2\text{PO}_4$

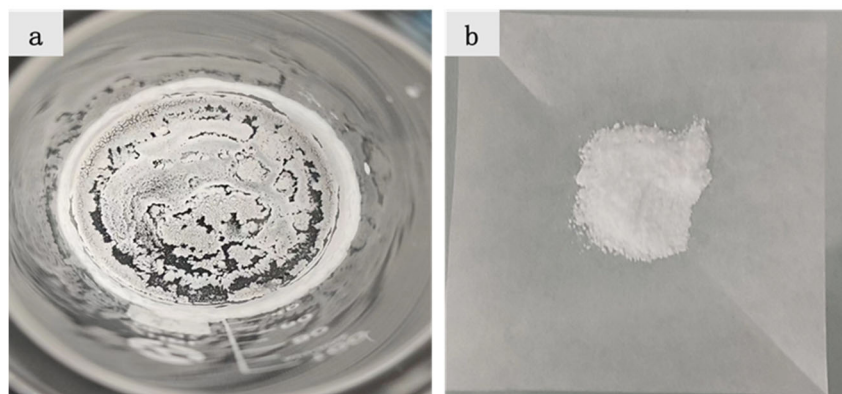


Figure 2. (a) Li<sub>3</sub>PO<sub>4</sub> precipitation; (b) LiH<sub>2</sub>PO<sub>4</sub> white powder

## 2.2 Structural characterization of recovered LiH<sub>2</sub>PO<sub>4</sub>

### (1) XRD characterization and analysis

The product Li<sub>3</sub>PO<sub>4</sub> was characterized by XRD, and the results are shown in Figure 5.3. It can be seen from the figure that the product has a high degree of crystallization and no obvious impurity peaks, which correspond one-to-one with the characteristic peaks of the standard card (PDF # 25-1030), proving that the obtained product is Li<sub>3</sub>PO<sub>4</sub>.

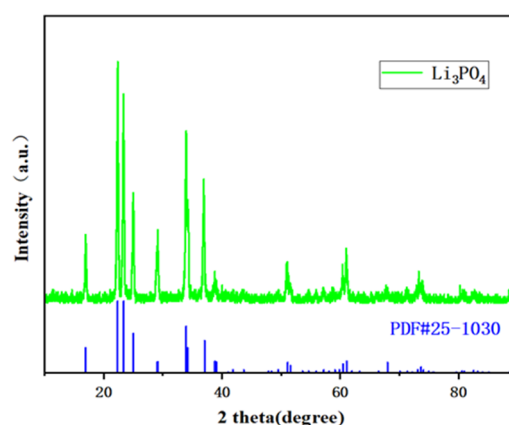


Figure3. Li<sub>3</sub>PO<sub>4</sub> XRD pattern

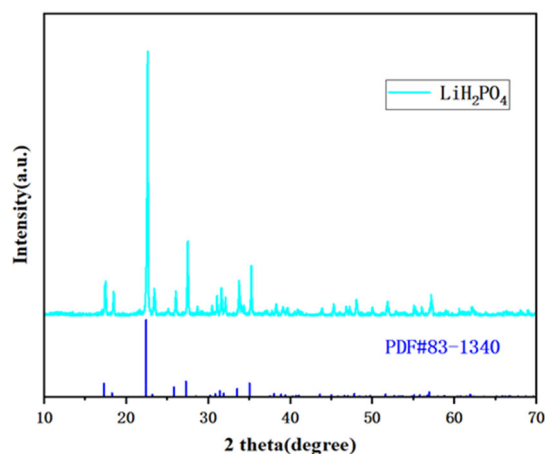


Figure4. LiH<sub>2</sub>PO<sub>4</sub> XRD pattern

The product LiH<sub>2</sub>PO<sub>4</sub> was characterized by XRD and compared with the standard card (PDF # 83-1340). The results are shown in Figure 4, where the characteristic peaks correspond one-to-one with a high degree of crystallinity and no obvious impurities, indicating that the obtained white product is LiH<sub>2</sub>PO<sub>4</sub>.

(2)SEM characterization and analysis of  $\text{LiH}_2\text{PO}_4$

Figure 5 shows the SEM image of  $\text{LiH}_2\text{PO}_4$  (10 $\mu\text{m}$ ) From the figure, it can be observed that the morphology of the obtained product is relatively regular and the particle distribution is relatively uniform, so it can be used as a raw material for synthesizing  $\text{LiFePO}_4$  precursors.

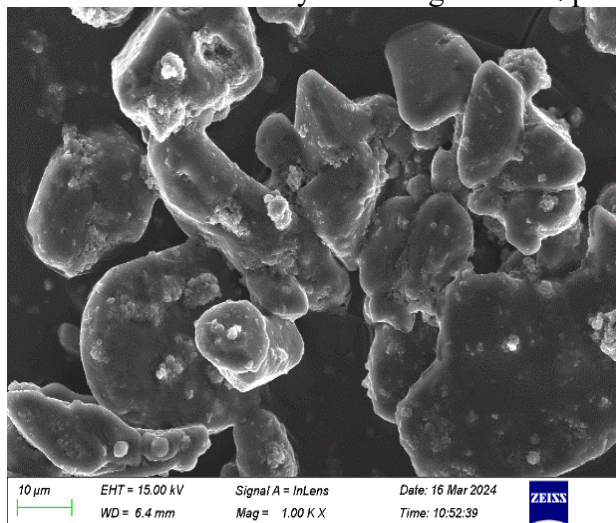


Figure 5. SEM photos of recycled  $\text{LiH}_2\text{PO}_4$

(3)Analysis of  $\text{LiH}_2\text{PO}_4$  Element Content (ICP)

Elemental analysis was performed on the recovered  $\text{LiH}_2\text{PO}_4$ , as shown in Table 1. It can be concluded that the actual content of Li and P is close to the theoretical content, indicating a higher purity of  $\text{LiH}_2\text{PO}_4$ .

Table 1. Results of  $\text{LiH}_2\text{PO}_4$  ICP Analysis

Detecting elements	Theoretical (W%)	Result (W%)
Li	6.7	6.4
p	29.8	26.5

3. Regeneration of  $\text{LiFePO}_4/\text{C}$  and optimization of conditions

The process flow of regenerating  $\text{LiFePO}_4/\text{C}$  using  $\text{LiH}_2\text{PO}_4$  as raw material is shown in Figure6.

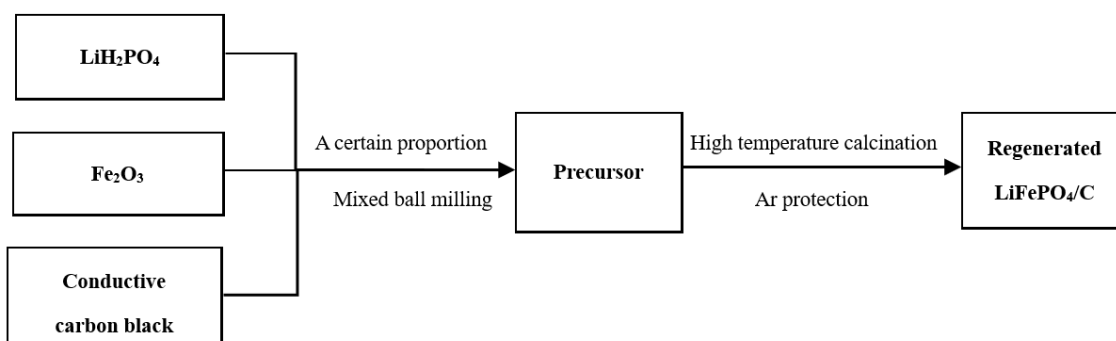


Figure 6. Process flow diagram of  $\text{LiFePO}_4/\text{C}$  regeneration using  $\text{LiH}_2\text{PO}_4$  as raw material

3.1 Regeneration of  $\text{LiFePO}_4$  cathode material

Using the recovered  $\text{LiH}_2\text{PO}_4$  as the lithium source and commercial  $\text{Fe}_2\text{O}_3$  as the iron source, with a molar ratio of  $\text{Li}:\text{Fe}=1.03:1$ , and adding 5% conductive carbon black as the carbon source, they are mixed together and packed into a ball milling tank. Anhydrous ethanol is used as a dispersant, and wet ball milling is carried out at a speed of 300r/min and a ball to material ratio of 20:1 for 6 hours. Then, the mixture is dried in a blast drying oven at 80°C. After grinding the dried powder for a period

of time, it is placed in an Ar protected tube furnace. The mixture is raised to 450°C at a rate of 5°C/min for 4 hours, and then raised to 450°C at a rate of 5°C/min. Maintain for 10 hours under conditions of 600°C、650°C、700°C、750°C、800°C, and regenerate carbon coated lithium iron phosphate cathode material (LiFePO<sub>4</sub>/C).

### 3.2 The Effect of Temperature on the Structure and Properties of Regenerated LiFePO<sub>4</sub>/C

XRD characterization and analysis of regenerated LiFePO<sub>4</sub>/C

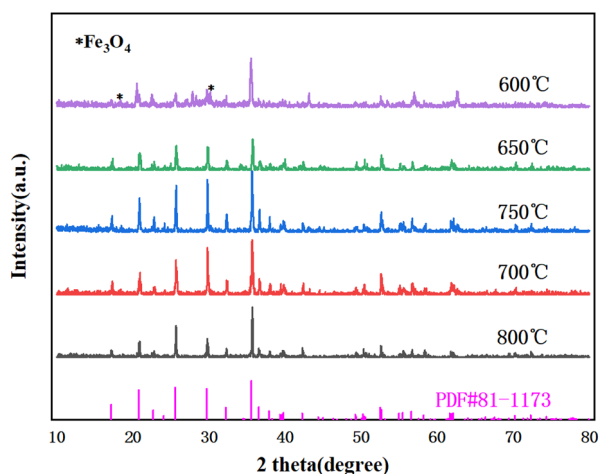


**Figure 7.** XRD patterns of LiFePO<sub>4</sub>/C regenerated by calcination at 600°C~800°C for 10 hours

Figure 7 shows the XRD pattern of LiFePO<sub>4</sub>/C samples regenerated after 10 hours of calcination at 600°C to 800°C. Thermodynamically, it is beneficial to reduce Fe<sup>3+</sup> to Fe<sup>2+</sup> at temperatures higher than 650°C. There are no obvious impurity peaks in the regenerated LiFePO<sub>4</sub> at different temperatures, and the characteristic peaks are consistent with the standard card of LiFePO<sub>4</sub> (PDF # 81-1173). As the temperature increases, the peak intensity becomes stronger, the peak shape becomes sharper, the half peak width narrows, and the degree of crystallization also increases.

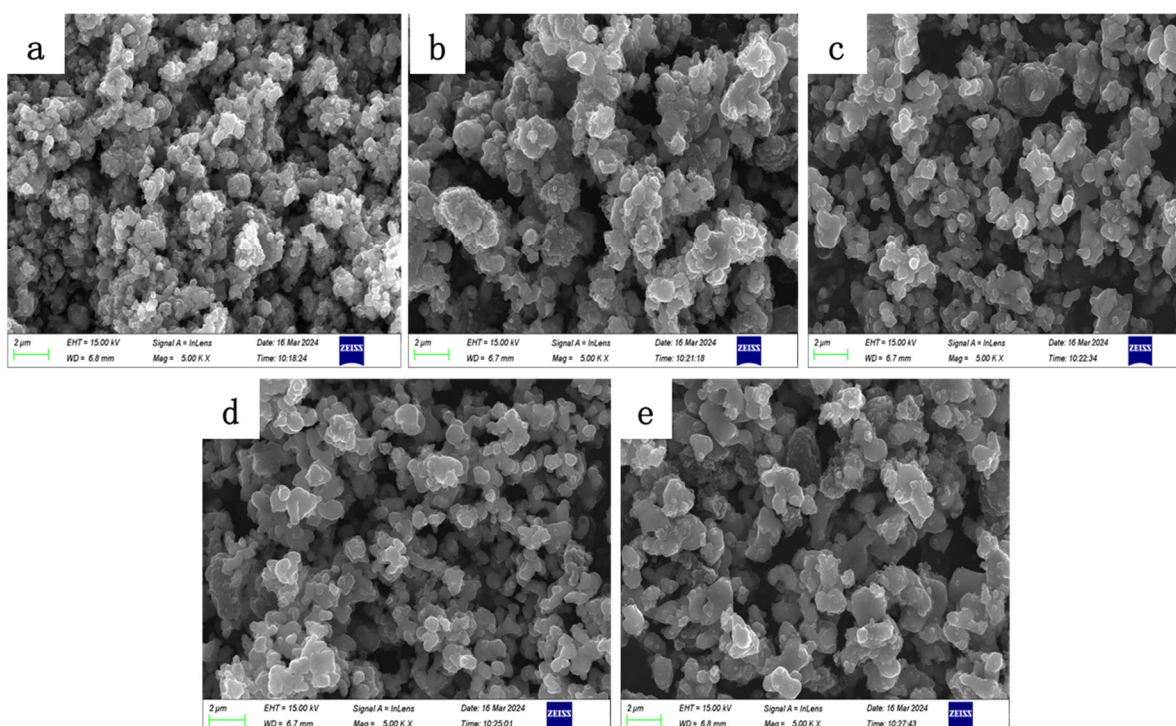
#### (2) SEM characterization and analysis of regenerated LiFePO<sub>4</sub>/C

Figure 7 shows SEM images of LiFePO<sub>4</sub> samples regenerated by calcination at 600°C~800°C for 10 hours with a conductive carbon black content of 5% in the precursor mixture (2 μm). From the graph, it can be seen that as the calcination temperature increases, the material particles also continuously increase in size; From the figure (d), it can be seen that the particle distribution is relatively uniform at 750°C, and the particle size is moderate, with a particle size of 1 μm. Around m, the morphology is relatively regular; At 600°C, the particles are small and there is some agglomeration between them, and the morphology is uneven; At 650°C and 700°C, a significant increase in the number of large particles can be observed; At 800°C, the largest number of large particles can be observed, and there is also a significant agglomeration phenomenon between the particles.

In order to investigate the effect of calcination temperature on material properties, the first cycle charge discharge curves of LiFePO<sub>4</sub>/C regenerated at calcination temperatures of 600°C~800°C were tested. Figure 9 (b) shows the first cycle charge discharge curves of LiFePO<sub>4</sub>/C regenerated at different calcination temperatures at a rate of 0.1C. It can be seen from the figure that the difference in charge discharge voltage plateau of the regenerated materials at these temperatures is very small, and the polarization phenomenon is not obvious. At a rate of 0.1C, the first cycle discharge capacities of LiFePO<sub>4</sub>/C regenerated at 600°C、650°C、700°C、750°C、800°C were 95.7mAh/g、117.8mAh/g、121.1mAh/g、125.7mAh/g、114.3mAh/g, respectively. The variation of discharge specific capacity with temperature is shown in Figure 9 (a). As the temperature increases, the first cycle discharge specific capacity first increases and then decreases. As the temperature increases, the

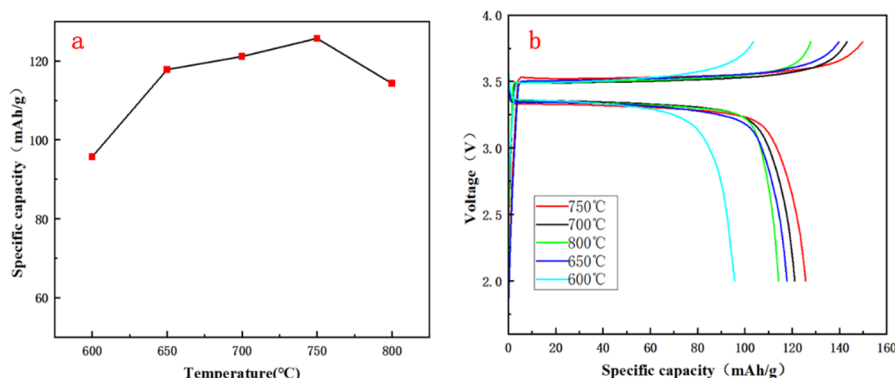
degree of crystallinity of material particles continuously increases, and the particle distribution becomes more uniform, which is conducive to the deintercalation of  $\text{Li}^+$  and improves the electrochemical performance of the material; When the temperature is too high, the particle size becomes too large and the agglomeration phenomenon becomes obvious, which is not conducive to the deintercalation of  $\text{Li}^+$ ; The calcination temperature should not be too high or too low.

Figure 10 shows the cyclic performance curve of  $\text{LiFePO}_4/\text{C}$  regenerated at a 1C rate from  $600^\circ\text{C}$  to  $800^\circ\text{C}$ . Combined with Table 2, it can be seen that there is a significant difference in the cyclic performance of  $\text{LiFePO}_4/\text{C}$  regenerated at  $600^\circ\text{C}$  to  $800^\circ\text{C}$ . At  $600^\circ\text{C}$ , the discharge specific capacity is low, and under 1C rate conditions, the first week discharge specific capacity is only  $82.4\text{mAh/g}$ . The reason, combined with the XRD and SEM characterization above, is that the temperature is too low to fully carry out the oxidation-reduction reaction, and  $\text{Fe}^{3+}$  cannot be completely reduced to  $\text{Fe}^{2+}$ , which will introduce iron impurities such as  $\text{Fe}_3\text{O}_4$  to reduce the electrochemical performance of the material; When the calcination temperature is at  $650^\circ\text{C}$ ,  $700^\circ\text{C}$ ,  $750^\circ\text{C}$ , the first week discharge specific capacity of the material continuously increases under 1C rate conditions. This is mainly because as the temperature increases, the crystallinity of  $\text{LiFePO}_4/\text{C}$  continues to increase, the particle morphology becomes more regular, and the dispersion degree between particles also becomes more uniform. Therefore, the cycling performance of  $\text{LiFePO}_4/\text{C}$  regenerated at  $750^\circ\text{C}$  is relatively good. The material has a first discharge specific capacity of  $106.2\text{mAh/g}$  under 1C rate conditions, and a discharge specific capacity of  $93.1\text{mAh/g}$  after 100 weeks, with a capacity retention rate of 87.7%; The cycling performance of  $\text{LiFePO}_4/\text{C}$  regenerated at  $800^\circ\text{C}$  is poor. Under 1C rate conditions, the first week discharge specific capacity is only  $86.2\text{mAh/g}$ , and the 100th week discharge specific capacity is  $75.2\text{mAh/g}$ . The reason is that the material particles calcined at  $800^\circ\text{C}$  have a larger particle size, which increases the diffusion path of  $\text{Li}^+$  and reduces the diffusion rate of  $\text{Li}^+$ ; Moreover, excessively high temperatures can lead to strong reducibility of C, which may result in the generation of a small amount of  $\text{Fe}_2\text{P}$ . The generation of  $\text{Fe}_2\text{P}$  will consume a portion of  $\text{LiFePO}_4$ <sup>[15]</sup>, resulting in a decrease in active substances and a decrease in the electrochemical performance of the material. Overall comparison shows that the electrochemical performance of the material is relatively good at  $750^\circ\text{C}$ .



**Figure 8.** SEM images of  $\text{LiFePO}_4$  synthesized at different temperatures: (a)  $600^\circ\text{C}$ ; (b)  $650^\circ\text{C}$ ; (c)  $700^\circ\text{C}$ ; (d)  $750^\circ\text{C}$ ; (e)  $800^\circ\text{C}$

(3)Electrochemical performance testing



**Figure 9.** (a) the first-week charge-discharge curve of LiFePO<sub>4</sub>/C regenerated at 600°C~800°C: (b) the first-week charge-discharge curve of LiFePO<sub>4</sub>/C regenerated at 600°C~800°C

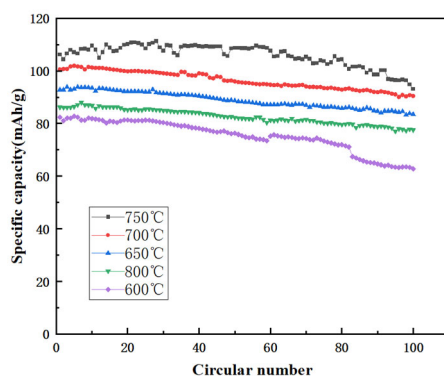


**Figure 10.** Cycle characteristic curve of LiFePO<sub>4</sub>/C regenerated at 600°C~800 °C at 1C magnification

**Table 2.** Cycle performance of LiFePO<sub>4</sub>/C regenerated at 600°C~800°C at 1C magnification

temperature(°C)	Multiplier(C)	First week discharge specific capacity(mAh/g)	Discharge specific capacity after the 100th week (mAh/g)	Capacity retention rate (%)
600	1	82.4	62.8	76.2
650	1	92.8	83.2	89.7
700	1	100.5	90	89.6
750	1	106.2	93.1	87.7
800	1	86.2	75.2	87.3

#### 4. Conclusion

This chapter provides a detailed introduction to the preparation process of LiFePO<sub>4</sub>/C material regeneration using recycled LiH<sub>2</sub>PO<sub>4</sub> as raw material. The product LiH<sub>2</sub>PO<sub>4</sub> recovered from waste lithium iron phosphate batteries has good crystallinity, regular particle morphology, and uniform distribution, providing raw materials for the regeneration of LiFePO<sub>4</sub>/C. In order to determine the optimal conditions for the electrochemical performance of regenerated LiFePO<sub>4</sub>/C, this chapter explores temperature as the main influencing factor.

In the study of electrochemical performance of regenerated LiFePO<sub>4</sub>/C under different temperature conditions, the study temperature was between 600°C to 800°C. The experimental results showed that the particle size of regenerated LiFePO<sub>4</sub>/C was moderate and the distribution was relatively uniform

under 750°C conditions. The electrochemical performance of regenerated LiFePO<sub>4</sub>/C was the best, with a first cycle discharge specific capacity of 125.7mAh/g at a 0.1C rate and good cycling performance; The initial discharge capacity of the material under 1C rate conditions is 106.2mAh/g, and the specific discharge capacity after the 100th week is 93.1mAh/g, with a capacity retention rate of 87.7%.

## Acknowledgements

This work was supported by the Jiangxi Provincial Education Department Project (No. GJJ211915; No. GJJ211913; GJJ190952), the National Natural Science Foundation of China (No. 22269014).

## References

- [1] Tang Weijian, Zhang Weixin, Yang Zeheng, et al. 2020 Research progress in the preparation and modification of LiFePO<sub>4</sub> cathode materials Power Technology [J], 44: 1077-1085
- [2] Zhang W-J 2011. Structure and performance of LiFePO<sub>4</sub> cathode materials: A review. Journal of Power Sources [J], 196: 2962-2970.
- [3] Padhi, A. K 1997. Phospho-olivines as Positive-Electrode Materials for Rechargeable Lithium Batteries. Journal of The Electrochemical Society [J], 144: 1188-1194.
- [4] Zhang Bangsheng, Liu Guiqing, Wang Fang, et al. 2020 Market Analysis of Waste Power Battery Recycling in 2020 Comprehensive utilization of resources in China [J], 38:102-105
- [5] Chen M, Ma X, Chen B, et al. 2019. Recycling End-of-Life Electric Vehicle Lithium-Ion Batteries. Joule [J], 3: 2622-2646.
- [6] Richa K, Babbitt C W, Gaustad G, et al. 2014. A future perspective on lithium-ion battery waste flows from electric vehicles. Resources Conservation & Recycling [J], 83: 63-76.
- [7] Xu X, Hu W, Liu W, et al. 2021. Study on the economic benefits of retired electric vehicle batteries participating in the electricity markets. Journal of cleaner production [J], 286: 125414.125411-125414.125414.
- [8] Xu P, Dai Q, Gao H, et al. 2020. Efficient Direct Recycling of Lithium-Ion Battery Cathodes by Targeted Healing. 4: 2609-2626.
- [9] Wang Fang 2020 Research on Lithium Mineral Resources [M]
- [10] Ma Zhe, Li Jianwu 2018 Research on China's Lithium Resource Supply System: Current Status, Problems, and Suggestions China Mining [J], 27:1-7
- [11] Zhang Sujiang, Zhang Yanwen, Zhang Liwei, et al. 2020 The current situation of lithium resources in China and its sustainable development strategies Inorganic salt industry [J], 52:1-7
- [12] Harper G, Sommerville R, Kendrick E, et al. 2019. Recycling lithium-ion batteries from electric vehicles. Nature [J], 575: 75-86.
- [13] Chen Yongzhen, Li Hualing, Song Wenji, et al. 2018 Solid phase regeneration and electrochemical performance study of waste lithium iron phosphate materials Journal of Chemical Engineering [J], 69: 5316-5325
- [14] Yao Kailin Research on the preparation method and application of battery grade lithium dihydrogen phosphate [C]//
- [15] Wang Qiang, Zeng Hui, Wang Kangping, 2015 The effect of lithium iron phosphate sintering process on the generation of iron phosphide Battery [J], 45:209-211.